Decoupling between upper crustal deformation of southern Tibet and underthrusting of Indian lithosphere

Shiguang Wang, Anne Replumaz, Marie-luce Chevalier, Haibing Li

Decoupling between upper crustal deformation of southern Tibet and underthrusting of Indian lithosphere

Terra Nova, doi: 10.1111/ter.12563, 2021

Shiguang Wang[1,2], Anne Replumaz[3], Marie-Luce Chevalier[2,4*], Haibing Li[2,4]

1. National Institute of Natural Hazards, Ministry of Emergency Management of China, 1 Anningzhuang Rd, Beijing 100085, China. 376792081@qq.com
2. Key Laboratory of Deep-Earth Dynamics of Ministry of Natural Resources, Institute of Geology, Chinese Academy of Geological Sciences, 26 Baiwanzhuang Rd, Beijing 100037, China. mlchevalier@hotmail.com, lihaibing06@163.com
3. ISTerre, Université Grenoble Alpes, CNRS, Grenoble, France. anne.replumaz@univ-grenoble-alpes.fr
4. Southern Marine Science and Engineering Guangdong Laboratory (Guangzhou), Guangzhou 511458, China

Short title: Upper crustal deformation of southern Tibet

* Corresponding author: Marie-Luce Chevalier, E-mail: mlchevalier@hotmail.com, Tel: +8613466654223

Statement of significance

In the India-Asia collision compressive context, surprising dominant east-west extension is observed in southern Tibet, expressed as large north-south-trending rifts. Whether such upper crustal extension is due to underthrusting of India (i.e., Indian lower crust + lithospheric mantle, bending beneath the Himalayan range and flattening below southern Tibet) or in-plane forces arising from the Indian indenter, is highly debated. Here, we use P-waves global tomography images (at depths of ~200 km), that reveal the northern extent of the underthrust Indian plate beneath Tibet, to show that there is no correlation with the location of the rifts that dissect southern Tibet. On the contrary, as previously suggested, such strong east-west extension in southern Tibet is correlated to the curved shape of the Himalayan arc, limited to the north by a major en-echelon strike-slip fault zone joining the two extremities (syntaxes) of the arc. North of this zone however, weaker extension is observed, driven by southeastward extrusion of eastern Tibet, bounded by major east-trending strike-slip faults visible as strong discontinuities in the GPS velocity field. Therefore, we argue that extension in Tibet appears correlated to upper crustal arc and fault geometries, but decorrelated to underthrusting India underneath.

Abstract

More accurate normal fault mapping and more recently constrained extension rates in southern and central Tibet allow to better discuss the mechanical processes responsible for the distribution of extension in Tibet. First, we show that the location of the rifts in southern Tibet south of the Karakorum-Jiali fault zone (KJFZ) does not exactly correspond to that of the rigid Indian lower lithosphere flattening below southern Tibet (underthrusting) inferred by P-waves global tomography, thus suggesting an absence of mechanical coupling between the two processes. Instead, E-W extension south of the KJFZ appears primarily due to divergent, orthogonal thrusting along the curved Himalayan arc, as proposed earlier. North of the KJFZ however, lower amplitude extension, distributed on numerous scattered normal faults in the western Qiangtang terrane, absorbs distributed eastward extrusion, while eastern Qiangtang is extruded more rigidly by the Xianshuihe fault, following a slip-line resulting from in-plane forces due to the collision/indenter, visible as a major discontinuity in the GPS velocity field.

1. Introduction

Whether and how upper crustal deformation in mountainous regions is linked to processes at depth, in the lower crust and in the lithospheric mantle, has been debated for decades, leading to irreconcilable models of crustal deformation. In particular, how exactly has underthrusting of the Indian lower lithosphere (lower crust and upper mantle, flattening below Tibet) influenced Tibetan tectonics remains debated due to the unknown exact location of its northern extent beneath Tibet. Indeed, almost one century ago, it was first proposed that the Tibetan Plateau, with its uniformly high elevation and vast extent, formed due to India underthrusting most of Tibet (Argand, 1924). Since then, while S-waves tomography images, more accurate in the vertical direction, showed a large cold anomaly interpreted as Indian lithospheric mantle beneath most of Tibet (Griot et al., 1998; Priestley et al., 2006, 2008), P-waves tomography images, more accurate in the horizontal

direction, showed a smaller extent of the Indian lithosphere only beneath southern Tibet (e.g., Li et al., 2008; Replumaz et al., 2004, 2010, 2014), thus refuting a correlation with the high elevation of the plateau. Taking such more accurate extent, several numerical mechanical (e.g., Copley et al., 2011) and geologic (e.g., DeCelles et al., 2002; Kapp and Guynn, 2004; Styron et al., 2015) models have suggested that in southern Tibet, it is the underthrusting of India that drives the observed upper crustal extension (Fig. 1D), while in the eastern plateau, extension would be due to gravitational collapse of the high plateau, driven by buoyancy forces (e.g., Dewey, 1988; Clark and Royden, 2000; Copley, 2008) (Fig. 1E).

By contrast, upper crustal tectonic models are built on observation of upper crustal deformation, considered to arise from in-plane forces resulting from the collision/indenter (e.g., Tapponnier and Molnar, 1976; Peltzer and Saucier, 1996), with minor depth variation of strain and minor influence of the Indian lithospheric mantle beneath Tibet. These models focus on a correlation between the location of the south Tibetan rifts south of the KJFZ and the arcuate shape of the Himalaya, so that extension is driven by divergent, orthogonal thrusting along the curved Himalayan arc (Fig. 1A), in contrast to the Qiangtang block north of the KJFZ, which behaves as a rigid block that is extruded eastwards (e.g., Baranowski et al., 1984; Armijo et al., 1986, 1989). Other models later pointed out that ~N-S trending rifts also exist north of the KJFZ in the Qiangtang terrane, thus proposing that eastward motion of Qiangtang occurs through symmetrical, conjugate strike-slip faults of different senses on each side of the KJFZ (Fig. 1C), leaving a triangular basin at the trail end of the extruding wedge (Taylor et al., 2003). However, that rifts north of the KJFZ are significantly less prominent than those to the south led Han et al. (2019) to suggest that the Qiangtang terrane has undergone significant extension distributed on numerous scattered small faults (Fig. 1B), so that it can no longer be treated as an integral block.

In this paper, we summarize, test and discuss these models for southern and eastern Tibet deformation previously published by our group and others, by comparing the P-waves tomography

images of the extent of the underthrusting Indian lithosphere with the exact location of the south Tibetan rifts. We eventually propose an improved model for upper crustal deformation in southern and eastern Tibet.

2. Upper crustal deformation in southern and eastern Tibet from tectonic, GPS and earthquakes distribution

The state of stress within the plateau is correlated to elevation: large-scale thrusting and crustal thickening dominate the lower elevations surrounding the plateau, and a combination of strike-slip and normal faulting dominates the high plateau interior, as shown by focal mechanisms (e.g., Molnar and Lyon-Caen, 1989; Elliott et al., 2010). Chevalier et al. (2020) recently determined E-W extension rates along the most prominent south Tibetan rift (Yadong-Gulu) that are relatively uniform at 1.3±0.3 mm/yr between the Yarlung Zangbo suture and the Gulu bend (~30.6°N). Rates instead increase to 3-6 mm/yr at the northern termination of the rift close to the Beng Co right-lateral strike-slip fault, part of the KJFZ, where seismicity increases (Fig. 2C). Summing their average rate for each of the seven main south Tibetan rifts (Chevalier et al., 2012; Kali, 2010; Wu et al., 2004, 2015; Ha et al., 2019; Wang et al., 2020), they further suggested a total extension rate of 9±2 mm/yr between 81° and 92°E in southern Tibet (Chevalier et al., 2020). By contrast, extension rates from single rifts located north of the KJFZ are much smaller, <0.3 mm/yr (Blisniuk and Sharp, 2003; Pan et al., 2018; Liu et al., 2021), in agreement with their different morphologies hence kinematics (e.g., Chevalier et al., 2020). Note also that the directions of extension, perpendicular to the rift trends, are slightly different on each side of the KJFZ: WNW-ESE to the south and NW-SE to the north.

Taking the regional GPS velocity field in a Tibetan Plateau-fixed reference frame (e.g., Gan et al., 2007) interestingly highlights the existence of different tectonic blocks with rather clear boundaries, especially a southward motion near the Eastern Himalayan syntaxis (EHS), veering

to southeastward north of the Red River fault (Fig. 1B). In addition, a strong velocity gradient is observed in eastern Tibet across both the Xianshuihe and Kunlun faults, suggesting a strong localization of the deformation along those faults, consistent with fast (~10 mm/yr) left-lateral slip-rates at all timescales (e.g., Van der Woerd et al., 2002; Chevalier et al., 2017; Bai et al., 2018). By contrast, much less deformation is observed in the Songpan-Ganze terrane in between those two faults, except in the far east near the Longmen Shan thrust belt (Fig. 1B). Note however that the absence of GPS stations in western central Tibet also prevents a clear analysis of upper crustal deformation in those remote regions.

3. Lithospheric structure, from seismic profile and tomography data

Nábělek et al. (2009) and Wittlinger et al. (2009), by using an 800 km-long, densely spaced seismic array (Himalayan-tibetan Continental LIthosphere during Mountain Building, Hi-CLIMB project, see location in Fig. 2A) from India to roughly the KJFZ, constrained the lithospheric geometry beneath southern and central Tibet. They identified and interpreted a “double Moho” with a 15-km-thick layer in the middle, beneath the southern Lhasa terrane, as the underthrust Indian lower crust and lithospheric mantle, observed at least until 31°N beneath the Lhasa Moho. By contrast, at the western extremity of the Himalayan arc, seismic refraction/wide-angle reflection data (TIen shan—PAmir GEodynamic, TIPAGE project, see location in Fig. 2A) shows that Indian lithosphere underthrusts beneath Kohistan and the central Pamir until 38°20’N, reaching the southward Pamir subduction underlined by deep (>100 km) earthquakes (e.g., Mechie et al., 2012). Similar southward subduction of the Tarim craton beneath Tibet has been interpreted along the western end of the Altyn Tagh fault (Fig. 2C), underlined by shallower earthquakes between 50 and 100 km, with no interpretation of Indian lithosphere farther south (Wittlinger et al., 2004, Fig. 2A).

While such seismic profiles provide a 2D image of the crustal and lithospheric structures along discrete lines, tomography images obtained from P-waves arrival time data are far better to

map in 3D the lithospheric structures beneath the collision zone (Fig. 2). In particular, the thick positive (rapid, in blue) anomaly observed beneath India has been interpreted as the thick and cold Indian craton (marked as CR in Fig. 2B), continuing northwards as underthrusting India beneath Tibet (e.g., Li et al., 2008; Replumaz et al., 2010, 2014). Recent tomography images show that the northern extent of underthrusting India beneath Tibet decreases from west to east (blue dashed line in Fig. 2), with Indian lithosphere present till ~36°N beneath the entire (although narrow) Tibetan Plateau to the west (~78°E), to ~31°N in the center (~86°E), while to the east (~92°E), it only reaches the Yarlung Zangbo suture (YZS), in agreement with seismic profiles beneath the central (Nábělek et al., 2009; Wittlinger et al., 2009) and western (Mechie et al., 2012) Himalayas, also suggesting that Indian lithosphere may almost reach the Tarim slab (Wittlinger et al., 2004). While global tomography, which images the lithospheric structures beneath the entire Tibetan Plateau, is the most appropriate tool to test whether a correlation exists between underthrusting of India and the location of the south Tibetan rifts, quantitative measurements of the Indian slab extent are not yet possible due to the large uncertainties on the thermal and mineralogy structures of the Earth, so that interpretation is always done in a qualitative manner (e.g., Li et al., 2008). Note that interpretation will evolve with time as denser seismic data are obtained, so that the resulting resolution of the tomography images will also increase with time. In any case, comparing the position of the KJFZ, i.e., the northern extent of the south Tibetan rifts, with the northern extent of underthrusting India beneath Tibet (e.g., Li et al., 2008; Replumaz et al., 2010, 2013, 2014), shows an absence of correlation: to the west, as for the Thakkhola/Lopu Kangri rift (TKR/LKR) for instance, the underthrusting of India reaches beyond the northern part of the rift (Fig. 3A), while to the east as for the Yadong-Gulu rift (YGR) for example, the underthrusting of India does not reach the northern part of the rift (Fig. 3B).

4. Numerical mechanical model predictions of extension patterns in southern Tibet

Copley et al. (2011) explored the mechanical coupling (i.e., when mantle material and crust flow at the same velocity, Wang and Dixon, 2004) between the Tibetan upper crust and underthrust Indian crust to explain the difference in tectonic regime between normal faulting south of the KJFZ and strike-slip faulting with minor normal component north of it. Using a 3D numerical mechanical model of the Tibetan crust, reconstructing both type of faulting and motion at the surface (directly comparable to GPS data) by predicting the internal forces (stress field) within the crust, they concluded that such difference in faulting style is best explained by a strong mechanical coupling between India and the overlying Tibetan crust (Fig. 1D).

Other numerical models consider that the main driving forces are the buoyancy forces resulting from the high elevation and large crustal thickness of the Tibetan Plateau, generating an outward lower crustal viscous flow from the plateau center ("channel flow model"), hence a southward (e.g., Beaumont et al., 2004) and eastward (e.g. Clark and Royden, 2000) collapse of the plateau. In eastern Tibet, Copley (2008) built a 3D numerical mechanical model of the flow around the Sichuan Basin, predicting that at the eastern edge of the plateau, normal faulting should be perpendicular to the flow (parallel to the edge of the plateau) due to extension in the downslope direction where the topographic gradient is the largest, as expected for a collapse of the plateau, that eventually diverges south of the Sichuan Basin (Fig. 1E).

5. Comparison between the extent of underthrusting India, normal faulting patterns, and predictions of mechanical model

The model of Copley et al. (2011) suggests that the location of the rifts in southern Tibet coincides with a zone of mechanical coupling between the Tibetan upper crust and the underthrusting strong Indian lower crust, assumed to reach the KJFZ (black and white lines in Fig. 1D). However, the global P-waves tomography positive anomaly at the very shallow depth of 200

km (Li et al., 2008; Replumaz et al., 2013) reveals no correlation: to the west, underthrusting India reaches beyond the northern limit of the rifts while to the east, it does not reach the northern part of the rifts (Fig. 3). This lack of correlation suggests that crustal deformation in southern Tibet is not influenced by processes occurring at the lithospheric level.

Besides, while the direction of extension predicted by the model of Copley et al. (2011) south of the KJFZ, roughly E-W, is rather consistent with the direction of extension perpendicular to the trend of the rifts, WNW-ESE, the model predicts pure strike-slip faulting north of the KJFZ, while NW-SE extension is observed (Fig. 1D). Similarly, the direction of extension predicted from the outward crustal flow model in SE Tibet (Copley, 2008), parallel to the plateau's edge then diverging along the margin (Fig. 1E), is inconsistent with the actual direction of extension in SE Tibet observed along transtensive fault systems such as those of Litang (Chevalier et al., 2016) or Lijiang, which are oblique to the plateau's edge (Zhang et al., 2015).

6. Improvement for upper crustal models (tectonic models)

The tectonic model of Armijo et al. (1986), built only on observation of upper crustal deformation arising from in-plane forces due to the indenter, does not require a correlation with underthrusting of India, in agreement with what tomography images suggest. It has been proposed that only the upper crust thickens, not the mantle, so that such thickening must have been decoupled from a more rigid lower lithosphere underneath (Tapponnier et al., 2001). For the upper crust, this model proposed that the KJFZ corresponds to a large-scale, left-stepping en-echelon, right-lateral strike-slip fault zone that decouples motion between the crusts of northern and southern Tibet, allowing central Tibet's Qiangtang terrane to move eastward respective to India and southern Tibet (Fig. 1A). Such right-lateral shearing indeed occurs far enough north of the Himalayan arc so that eastward extrusion of central Tibet, between the KJFZ and the Altyn Tagh fault (Armijo et al., 1989), considered as mostly rigid (Peltzer and Saucier, 1996), can bypass the EHS. By contrast,

southern Tibet deforms in a divergent manner due to the curved shape of the Himalayan arc, generating extension through rifts confined within the arc curvature. That model requires that the ~EW extension rate observed across southern Tibet south of the KJFZ be about half that of divergent thrusting of rigid India beneath the Himalayan Range (Fig. 1A). Armijo et al. (1986) and more recently, Chevalier et al. (2020), indeed suggested a total extension rate of 9±2 mm/yr between 81 and 92°E across southern Tibet, which corresponds to half of the Holocene (e.g., 21 ± 1.5 mm/yr, Lavé and Avouac, 2000) and geodetic (19 ± 2.5 mm/yr in eastern Nepal, Bettinelli et al., 2006; or 15.5 ± 2 mm/yr, Lindsey et al., 2018) rates across the Himalaya.

However, shortcomings of Armijo et al. (1986, 1989)'s model are that considering central Tibet as a rigid block does not explain the presence of rifts in the Qiangtang terrane north of the KJFZ. However, given that rates of extension north of the KJFZ are only ~10-20% of those south of the KJFZ (e.g., Chevalier et al., 2020 and references therein) rules out upper crustal tectonic models suggesting that eastward motion occurs through symmetrical, conjugate strike-slip faults on each side of the KJFZ (Taylor et al., 2003; Yin et al., 2011). Instead, it has recently been proposed that eastward extrusion of the western and central parts of the Qiangtang terrane is absorbed by significant internal extension distributed on numerous scattered normal faults, so that it can no longer be treated as an integral block (Han et al., 2019). This internal deformation may be due to the absence of major strike-slip faults north of central Qiangtang, thus limiting efficient eastward extrusion (Fig. 4A). By contrast, rapid eastward motion of the eastern Qiangtang block is shown in the GPS velocity field by a large gradient across the Xianshuihe fault to the north and the Jiali fault to the SE, suggesting rigid block rotation around the EHS with strong localization of motion on strike-slip faults (Bai et al., 2018). At the scale of the Tibetan Plateau, Tapponnier and Molnar (1976) shown that such strike-slip faults follow slip-lines resulting from the Indian indenter collision forces. We thus re-draw a complete deformation pattern of the collision zone in agreement with the data synthesis we made in this study to suggest an improved model for upper crustal

deformation mechanisms of Tibet (Fig. 4). We conclude that upper crustal deformation in Tibet is driven by indentation of India, with strong extension due to divergent orthogonal thrusting along the curved Himalayan arc occurring south of the KJFZ, and eastward extrusion of the eastern and central parts of the Qiangtang terrane occurring between the KJFZ (allowing extrusion to bypass the EHS) and the Xianshuihe fault system, one of the major slip-line resulting from the indentation, with smaller extension in western Qiangtang where the Xianshuihe fault is not observed, distributed on numerous scattered normal faults (Fig. 4).

Acknowledgements

This project was financially supported by the second Tibetan Plateau Scientific Expedition of the Ministry of Science and Technology of China (2019QZKK0901), the Natural National Science Foundation of China (NSFC 41941016 and 42020104007), and the China Geological Survey (DD20190059).

References

Argand, E., 1924. La tectonique de l'Asie. 13th International Geological Congress, 171–372.

Armijo, R., Tapponnier, P., Mercier, J.L., and Han, T.L., 1986. Quaternary extension in southern Tibet: Field observations and tectonic implications. Journal of Geophysical Research, 91(B14), 13,803–13,872. https://doi.org/10.1029/JB091iB14p13803.

Armijo, R., Tapponnier, P., and Tonglin, H., 1989. Late Cenozoic right-lateral strike-slip faulting in southern Tibet. Journal of Geophysical Research, 94(B3), 2787–2838, doi:10.1029/JB094iB03p02787.

Bai, M., Chevalier, M.L., Pan, J., Replumaz, A., Leloup, P.H., Métois, M., and Li, H., 2018. Southeastward increase of the late Quaternary slip-rate of the Xianshuihe fault, eastern Tibet. Geodynamic and seismic hazard implications. Earth and Planetary Science Letters, 485, 19-31.

https://doi.org/10.1016/j.epsl.2017.12.045.

Baranowski, J., J. Armbruster, L. Seeber, and P. Molnar., 1984. Focal depths and fault plane solutions of earthquakes and active tectonics of the Himalayas. Journal of Geophysical Research, 89:6918-6928, 1984.

Beaumont, C., Jamieson, R.A., Nguyen, M.H. and Medvedev, S., 2004. Crustal channel flows: 1. Numerical models with applications to the tectonics of the Himalayan-Tibetan orogen. Journal of Geophysical Research, 109 (B6), B06406.

Bettinelli, P., Avouac, J.P., Flouzat, M., Jouanne, F., Bollinger, L., Willis, P., and Chitrakar, G.R., 2006. Plate Motion of India and Interseismic Strain in the Nepal Himalaya from GPS and DORIS Measurements. Journal of Geodesy, 80(8/11):567-589, doi: 10.1007/s00190-006-0030-3.

Blisniuk, P.M., and Sharp, W.D., 2003. Rates of late Quaternary normal faulting in central Tibet from U-series dating of pedogenic carbonate in displaced fluvial gravel deposits. Earth and Planetary Science Letters, 215(1–2), 169–186.

Chevalier, M.-L., Tapponnier, P., Van der Woerd, J., Ryerson, F.J., Finkel, R., and Li, H., 2012. Spatially constant slip rate along the southern segment of the Karakorum fault since 200 ka. Tectonophysics, 530-531(531), 152–179, 10.1016/j.tecto.2011.12.014.

Chevalier, M.L., Leloup, P.H., Replumaz, A., Pan, J., Liu, D., Li, H., Gourbet, L., and Métois, M., 2016. Tectonic-geomorphology of the Litang fault system, SE Tibetan Plateau, and implication for regional seismic hazard. Tectonophysics, 682, 278–292, doi:10.1016/j.tecto.2016.05.039.

Chevalier, M.L., Leloup, P.H., Replumaz, A., Pan, J., Metois, M., and Li, H., 2017. Temporally constant slip-rate along the Ganzi fault, NW Xianshuihe fault system, eastern Tibet. Geological Society of America Bulletin, 130(3/4), 396–410. https://doi.org/10.1130/B31691.1.

Chevalier, M.L., Tapponnier, P., van der Woerd, J., Leloup, P.H., Wang, S., Pan, J., Bai, M., Kali, E.,

Liu, X., and Li., H., 2020. Late Quaternary Extension Rates across the Northern Half of the Yadong-Gulu Rift–Implication for East-West Extension in Southern Tibet. Journal of Geophysical Research, 125. https://doi.org/10.1029/2019JB019106.

Clark, M.K. and Royden, L.H., 2000. Topographic ooze: Building the eastern margin of Tibet by lower crustal flow. Geology, 28 (8), 703-706.

Copley, A., 2008. Kinematics and dynamics of the southeastern margin of the Tibetan Plateau. Geophysical Journal International, 174(3), 1081-1100.

Copley, A., Avouac, J.P., and Wernicke, B.P., 2011. Evidence for mechanical coupling and strong Indian lower crust beneath southern Tibet. Nature, 472, 79–81, doi:10.1038/nature09926.

DeCelles, P.G., Robinson, D.M. and Zandt, G., 2002. Implications of shortening in the Himalayan fold-thrust belt for uplift of the Tibetan Plateau. Tectonics, 21(6), 12-1.

Dewey, J.F., 1988. Extensional collapse of orogens. Tectonics, 7(6), 1123-1139.

Elliott, J.R., Walters, R.J., England, P.C., Jackson, J.A., Li, Z., and Parsons, B., 2010. Extension on the Tibetan Plateau: Recent normal faulting measured by InSAR and body wave seismology. Geophysical Journal International, 183(2), 503–535. https://doi.org/10.1111/j.1365-246X.2010.04754.x.

Gan, W., Zhang, P., Shen, Z., Niu, Z., Wang, M., Wan, Y., and Cheng, J., 2007. Present-day crustal motion within the Tibetan Plateau inferred from GPS measurements. Journal of Geophysical Research, 112, B08416, doi:10.1029/2005JB004120.

Griot, D.A, Montagner, J.P., Tapponnier, P., 1998. Phase velocity structure from Rayleigh and Love waves in Tibet and its neighboring regions. Journal of Geophysical Research, 103, B9, 21,215-21,232.

Ha, G., Wu, Z., and Liu, F., 2019. Late Quaternary vertical slip rates along the Southern Yadong–Gulu Rift, Southern Tibetan Plateau. Tectonophysics, 755, 75–90. https://doi.org/10.1016/j.tecto.2019.02.014.

311 Han, S., Li, H., Pan, J., Lu, H., Zheng, Y., Liu, D., and Ge, C., 2019. Co-seismic surface ruptures
312 in Qiangtang Terrane: Insight into Late Cenozoic deformation of central Tibet.
313 Tectonophysics, 750, 359–378, doi :10.11016/j.tecto.2018.11.001.
314 Kali, E., 2010. De la déformation long-terme à court-terme sur les failles normales du Sud Tibet:
315 approche géochronologique multiméthodes (10Be, 26Al, (U-Th)/He, 40Ar/39Ar, U/Pb),
316 0–361, PhD thesis, EOS Strasbourg, France.
317 Kapp, P. and Guynn, J.H., 2004. Indian punch rifts Tibet. Geology, 32(11), 993-996.
318 Lavé, J. and Avouac, J.P., 2000. Active folding of fluvial terraces across the Siwaliks Hills,
319 Himalayas of central Nepal. Journal of Geophysical Research,105(B3):5735–5770,
320 10.1029/1999JB900292.
321 Li, C., van der Hilst, R.D., Meltzer, A.S., and Engdahl, E.R., 2008. Subduction of the Indian
322 lithosphere beneath the Tibetan Plateau and Burma. Earth and Planetary Science Letters, 274
323 (1-2), 157-168. http://dx.doi.org/10.1016/j.epsl.2008.07.016.
324 Lindsey, E.O., Almeida, R., Mallick, R., Hubbard, J., Bradley, K., Tsang, L.L.H., Liu, Y.,
325 Burgmann, R., and Hill, E.M., 2018. Structural Control on Down dip Locking Extent of the
326 Himalayan Megathrust. Journal of Geophysical Research, 123(6), 5265–5278.
327 doi:10.1029/2018jb015868.
328 Liu, F., Pan, J., Li, H., Sun, Z., Liu, D., Lu, H., Zheng, Y., Wang, S., Bai, M., Chevalier,
329 M.L., Zhang, L., Cao, Y., 2021. Characteristics of Quaternary Activities along the Riganpei
330 Co Fault and Seismogenic Structure of the July 23, 2020 Mw6.4 Nima Earthquake, Central
331 Tibet. Acta Geoscientica Sinica, doi: 10.3975/cagsb.2021.010402. (in Chinese with English
332 abstract).
333 Mechie, J., Yuan, X., Schurr, B., Schneider, F., Sippl, C., Ratschbacher, L.,Minaev, V., Gadoev, M.,
334 Oimahmadov, I., Abdybachaev, U., Moldobekov, B., Orunbaev, S., and Negmatullaev, S.,
335 2012. Crustal and uppermost mantle velocity structure along a profile across the Pamir and

336 southern Tien Shan as derived from project TIPAGE wide-angle seismic data. Geophysical
337 Journal International, 188, 385–407. http://dx.doi.org/10.1111/j.1365-246X.2011.05278.x.
338 Molnar, P., and Lyon-Caen, H., 1989. Fault plane solutions of earthquakes and active tectonics of
339 the Tibetan plateau and its margins. Geophysical Journal International, 99:123-153.
340 Nábělek, J., Hetényi, G., Vergne, J., Sapkota, S., Kafle, B., Jiang, M., Su, H., Chen, J., Huang, B-S,
341 and the Hi-CLIMB Team, 2009. Underplating in the Himalaya-Tibet collision zone revealed
342 by the Hi-CLIMB experiment. Science, 325, doi: 10.1126/science.1167719.
343 Pan, J., Li, H., Sun, Z., Liu, D., Lu, H., Zheng, Y., and Chevalier, M.L., 2018. Reassessment of the
344 late Quaternary slip rate of the Shuanghu graben, central Tibet, AGU Fall Meeting.
345 Peltzer, G., and Saucier, F., 1996. Present-day kinematics of Asia derived from geologic fault
346 rates. Journal of Geophysical Research, 101, 27,943–27,956.
347 Priestley, K., Debayle, E., McKenzie, D., and Pilidou, S., 2006. Upper mantle structure of eastern
348 Asia from multimode surface waveform tomography. Journal of Geophysical Research, 111,
349 B10304. http://doi:10.1029/2005JB004082.
350 Priestley, K., J. Jackson, and D. McKenzie., 2008. Lithospheric structure and deep earthquakes
351 beneath India, the Himalaya and southern Tibet, Geophysical Journal International, 172,
352 345–362. http://doi:10.1111/j.1365-246X.2007.03636.x.
353 Replumaz, A., Karason,H., van derHilst, R.D., Besse, J., Tapponnier, P., 2004. 4-D evolution of
354 SE Asia's mantle from geological reconstructions and seismic tomography. Earth and
355 Planetary Science Letters, 221, doi: 10.1016/s0012-821x(04)00070-6.
356 Replumaz, A., Negredo A.M., Villaseñor A. and Guillot S., 2010. Indian continental subduction and
357 slab break-off during Tertiary Collision. Terra Nova, 22, 290-296.
358 http://doi:10.1111/j.13653121.2010.00945.x
359 Replumaz, A., Guillot, S., Villaseñor, A., Negredo, A.M., 2013. Amount of Asian lithospheric
360 mantle subducted during the India/Asia collision. Gondwana Research 24, 936–945, doi:

10.1016/j.gr.2012.07.019.

Replumaz, A., Capitanio, F.A., Guillot, S., Negredo, A.M., and Villaseñor, A., 2014. The coupling of Indian subduction and Asian continental tectonics. Gondwana Research, 26, 608-626. http://doi:10.1016/j.gr.2014.04.003.

Styron, R., Taylor, M. and Sundell, K., 2015. Accelerated extension of Tibet linked to the northward underthrusting of Indian crust. Nature Geoscience, 8(2), 131-134.

Tapponnier, P, and Molnar, P., 1976. Slip line field theory and large-scale continental tectonics. Nature, 264, 319-324.

Tapponnier, P., Xu Z., Roger, F., Meye,r B., Arnaud, N., Wittlinger, G., and Yang, J., 2001. Oblique stepwise rise and growth of the Tibet plateau, Science, 294 (5547), 1671–1677. http://doi:10.1126/science.105978.

Taylor, M., Yin, A., Ryerson, F. J., Kapp, P., and Ding, L., 2003. Conjugate strike-slip faulting along the Bangong-Nujiang suture zone accommodates coeval east-west extension and north-south shortening in the interior of the Tibetan Plateau. Tectonics, 22(4), 1044, doi : 10.1029/2002TC001361.

Tilmann, F., Ni, J., Indepth III Seismic Team, 2003. Seismic imaging of the downwelling Indian lithosphere beneath Central Tibet. Science 300, 1424–1427.

Van Der Woerd, J., Tapponnier, P., Ryerson, F. J., Meriaux, A. S., Meyer, B., Gaudemer, Y., et al., 2002. Uniform postglacial slip-rate along the central 600 km of the Kunlun Fault (Tibet), from 26Al, 10Be, and 14C dating of riser offsets, and climatic origin of the regional morphology. Geophysical Journal International, 148(3), 356–388. https://doi.org/10.1046/j.1365-246x.2002.01556.x

Wang, K., and Dixon,T., 2004. “Coupling” Semantics and science in earthquake research. EOS, Transactions American Geophysical Union, 85(15),180.

Wang, S., Chevalier, M.L., Pan, J., Bai, M., Li, H., Li, K., and Wang, G., 2020. Late Quaternary

activity of the southern Yadong-Gulu rift, southern Tibet. Tectonophysics, 790, doi :10.1016/j.tecto.2020.228545.

Wittlinger, G., Vergne, J., Tapponnier, P., Farra, V., Poupinet, G., Jiang, M., Su, H., Herquel, G., and Paul, A., 2004. Teleseismic imaging of subducting lithosphere and Moho offsets beneath western Tibet, Earth and Planetary Science Letters, 221, 1–4, 117-130, Doi:10.1016/S0012-821X(03)00723-4.

Wittlinger, G., Farra, V., Hetényi, G., Vergne, J., and Nábělek, J., 2009. Seismic velocities in southern tibet lower crust: a receiver function approach for eclogite detection. Geophysical Journal of the Royal Astronomical Society, 177(3), 1037-1049.

Wu, Z., Zhao, X., Wu, Z., Jiang, W., Hu, D., and Zhou, C., 2004. Quaternary geology and faulting in the Damxung-Yangbajain basin. Acta Geologica Sinica, 78(1), 273–282.

Wu, Z., Ye, P., Wang, C., Zhang, K., Zhao, H., Zheng, Y., Yin, J., and Li, H., 2015. The relics, ages and significance of prehistoric large earthquakes in the Angang graben in South Tibet. Earth Science—Journal of China University of Geosciences, 40(10), 1621. https://doi.org/10.3799/dqkx.2015.147. (in Chinese with English abstract)

Yin, A., and Taylor, M.H., 2011. Mechanics of V-shaped conjugate strike-slip faults and the corresponding continuum mode of continental deformation. Geological Society of America Bulletin, 123, 9/10, 1798–1821, doi: 10.1130/B30159.1.

Zhang, Y., Replumaz, A.,Wang, G., Leloup, P.H., Gautheron, C., Bernet, M., van der Beek, P., Paquette, J.L.,Wang, A., Zhang, K., Chevalier, M.L., and Li, H., 2015. Timing and rate of exhumation along the Litang fault system, implication for fault re-organisation in South East Tibet. Tectonics, 34 (6), 1219-1243. http://dx.doi.org/10.1002/2014TC003671.

Figures

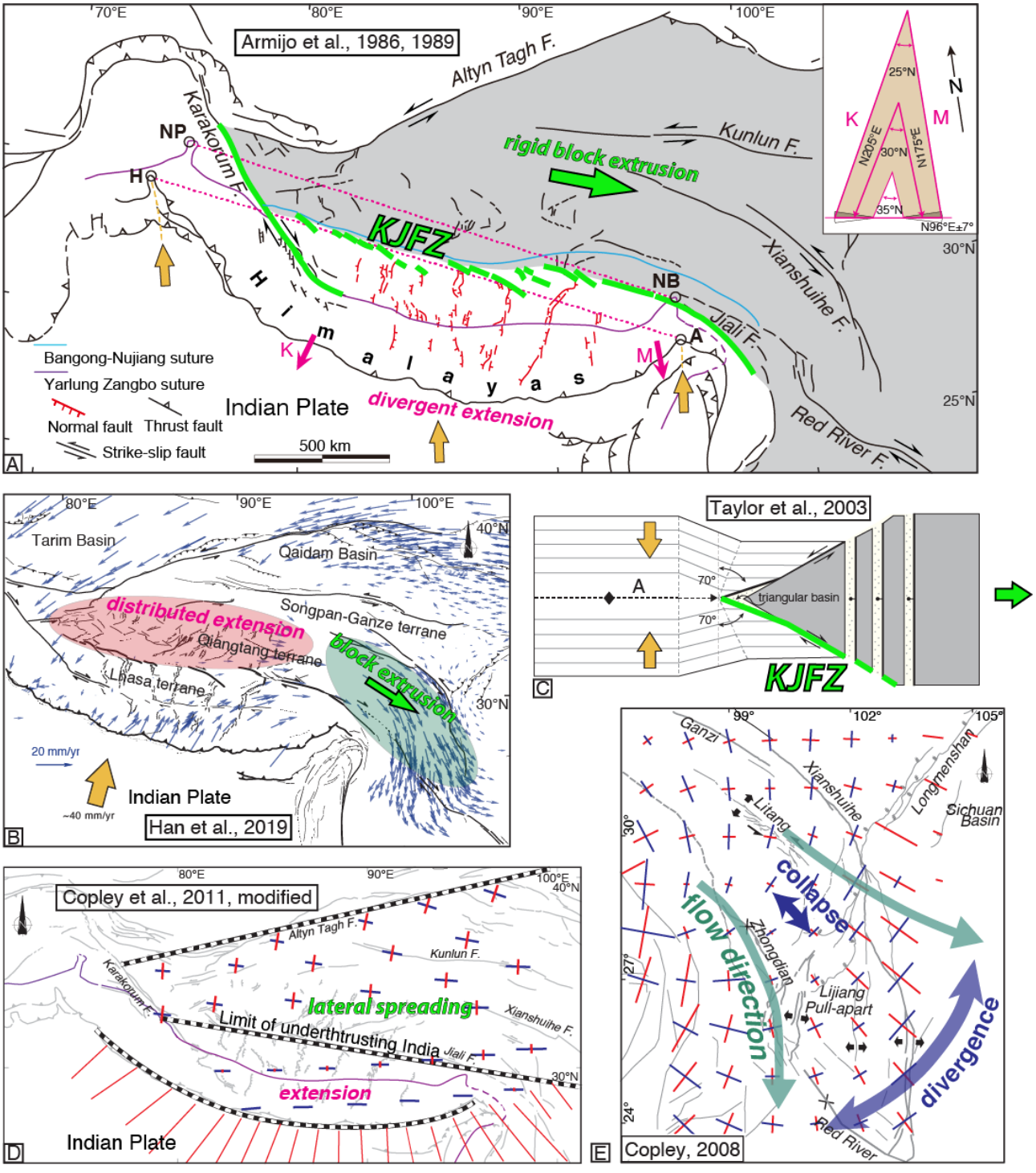

Figure 1: *Upper crustal tectonic (A, B and C) and numerical mechanical (D and E) models for Tibet. (A) Armijo et al. (1986, 1989)'s model, with eastward extrusion of central Tibet (grey-shaded) north of Karakorum-Jiali fault zone (KJFZ, a series of discontinuous, en-echelon strike-slip fault segments), and divergent deformation of southern Tibet due to curved shape of Himalayan arc. Rifts (in red) are confined between two vectors perpendicular to the arc, 'K' and 'M'. KJFZ in between western (H = Hazara, NP = Nanga Parbat) and eastern (A = Assam, NB = Namche Barwa)*

Himalayan syntaxes (pink dashed lines). (B) Han et al. (2019)'s model, with rifts north of KJFZ interpreted as extension distributed on numerous scattered small faults. GPS velocities relative to Tibetan Plateau from Gan et al. (2007). (C) Taylor et al. (2003)'s model, with eastward motion of Qiangtang occurring through symmetrical, conjugate strike-slip faults of different senses on each side of KJFZ. (D) Copley et al. (2011)'s model with principal axes of upper crustal horizontal strain-rate tensors (blue: extension; red: compression, both as crosses: strike-slip) due to Indian rigid lower crust (south of central black and white line), modified to fit Altyn Tagh fault (northern line) and Main Frontal thrust (southern line). (E) Copley (2008)'s model of upper crustal horizontal strain-rate tensors for SE Tibet, predicting extension perpendicular to SE edge of plateau due to gravitational collapse.

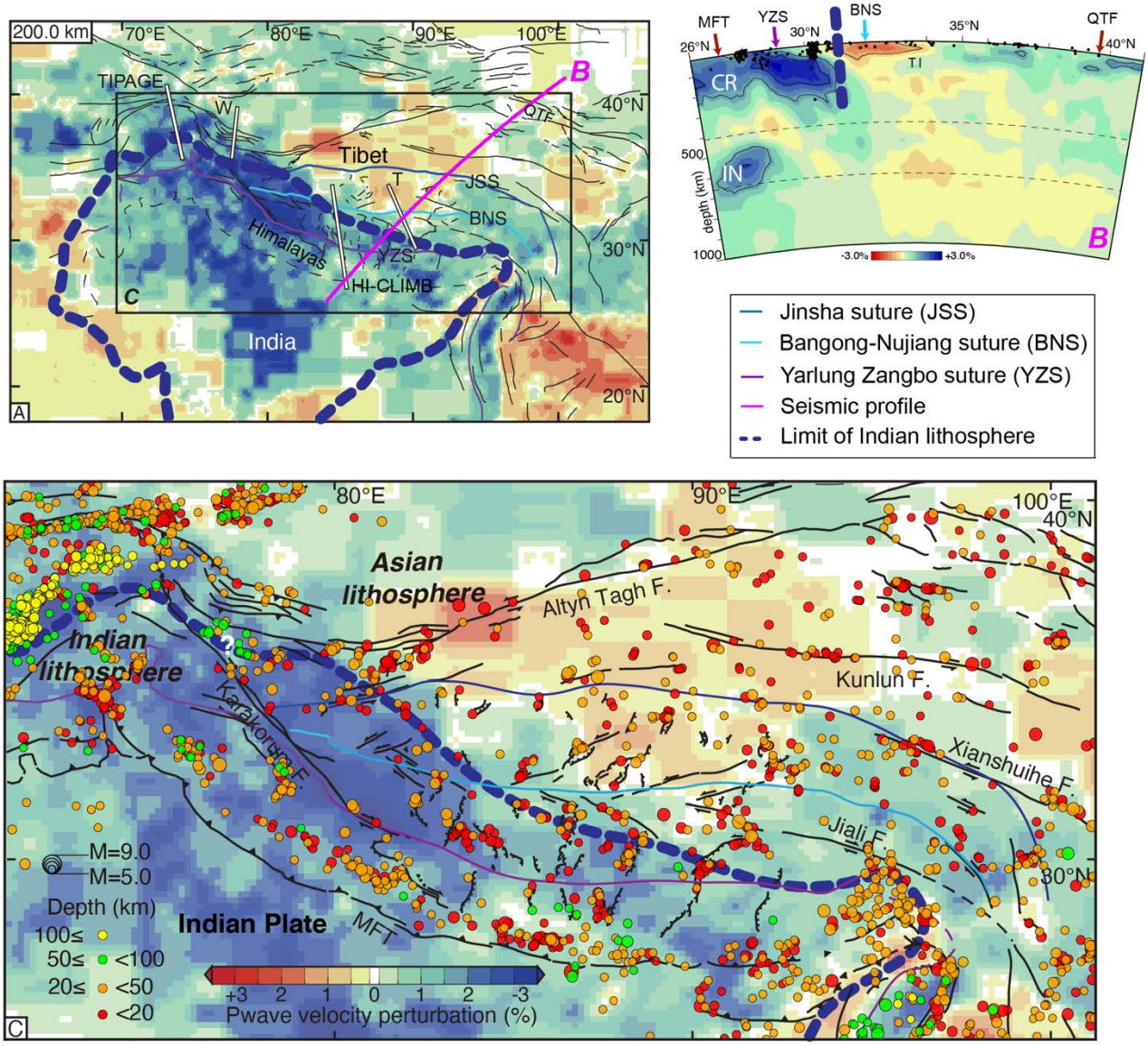

Figure 2: *(A) P-waves global tomography images at 200 km depth from Replumaz et al. (2013), with location of seismic profiles (in white) TIPAGE (Mechie et al., 2012), W=Wittlinger et al. (2004), HI-CLIMB (Nábělek et al., 2009) and T=Tilmann et al. (2003). QTF = Qilian Shan thrust fault, MFT = Main Frontal thrust. (B) Tomography cross-section (location shown in A). CR = Indian craton, IN = India, TI = Tibet. (C) Close-up with distribution of Mw≥5.0 earthquakes since 1900 (USGS), according to their depths.*

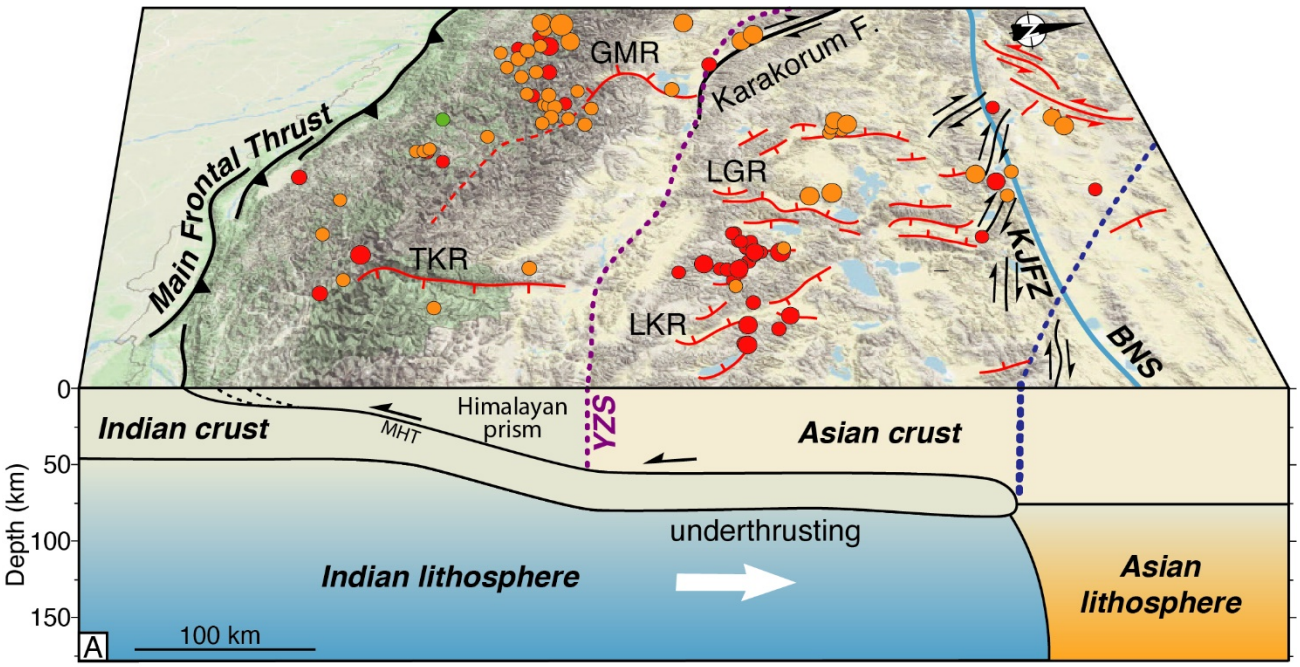
GMR
Karakorum F.
Main Frontal Thrust
LGR
TKR
KJFZ
LKR
BNS
0
Himalayan prism
MHT
YZS
Indian crust
Asian crust
50
Depth (km)
100
underthrusting
Indian lithosphere
Asian lithosphere
150
A
100 km

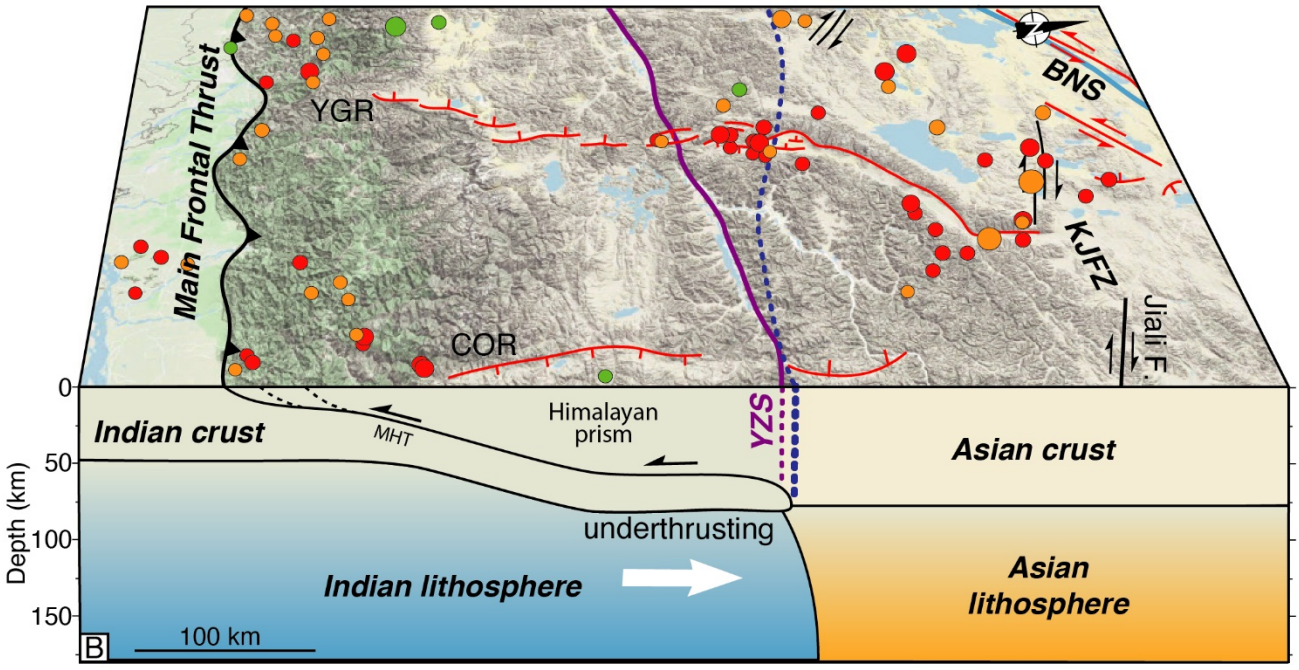
YGR
Main Frontal Thrust
BNS
KJFZ
Jiali F.
COR
0
Himalayan prism
MHT
YZS
Indian crust
Asian crust
50
Depth (km)
100
underthrusting
Indian lithosphere
Asian lithosphere
150
B
100 km

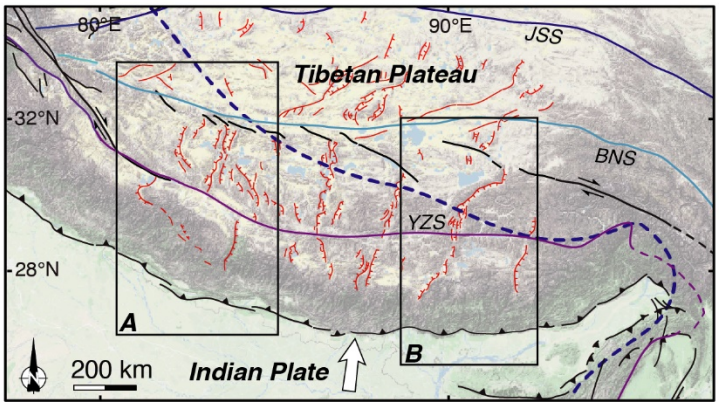
80°E
90°E
JSS
Tibetan Plateau
32°N
BNS
YZS
28°N
A
B
200 km
Indian Plate

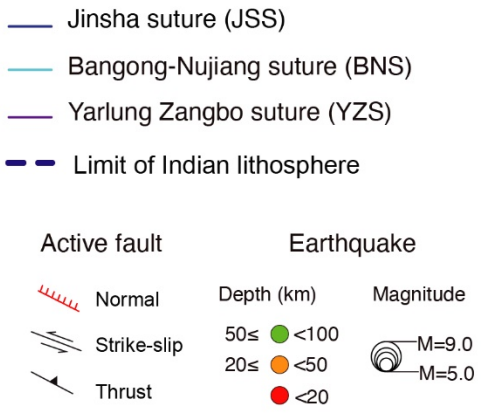
Jinsha suture (JSS)
Bangong-Nujiang suture (BNS)
Yarlung Zangbo suture (YZS)
Limit of Indian lithosphere
Active fault
Normal
Strike-slip
Thrust
Earthquake
Depth (km)
50≤ <100
20≤ <50
<20
Magnitude
M=9.0
M=5.0

435

Figure 3: *3D cartoon of western (A) and central (B) southern Tibet showing underthrusting of India, as well as active fault traces and Mw≥5.0 earthquakes (as in Fig. 2C). Dashed blue line represents northern extent of Indian lithosphere, deduced from P-waves global tomography as shown in Figure 2. GMR = Gurla Mandhata rift, TKR = Thakkhola, LGR = Lunggar, LKR = Lopu Kangri, YGR = Yadong-Gulu, COR = Cona-Oiga, MHT = Main Himalayan thrust, KJFZ = Karakorum-Jiali fault zone.*

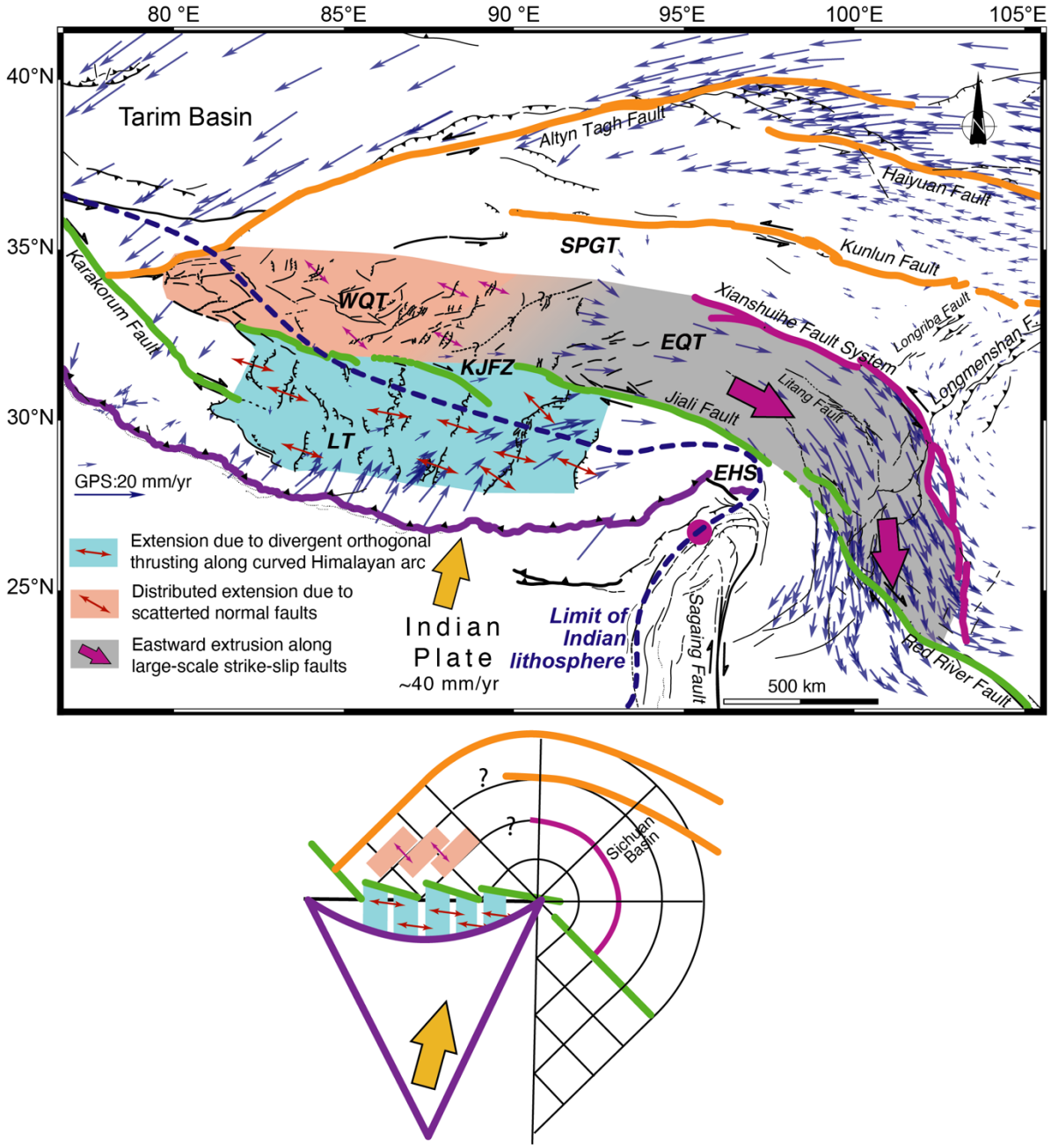

Figure 4: *Top: Kinematics of active tectonics in Tibet with GPS velocities relative to Tibetan Plateau (Gan et al., 2007). Red double-headed arrows show ESE-oriented extensional deformation in Lhasa terrane (LT) and purple ones show NW-SE extension in west-central Qiangtang terrane (WQT). Purple arrow to east indicates eastward extrusion along Xianshuihe fault and KJFZ of east-central Qiangtang terrane (EQT). Purple solid circle represents rotation pole of Eastern Himalayan Syntaxis (EHS). KJFZ = Karokorum-Jiali Fault Zone, SPGT = Songpan-Ganzi terrane. Bottom: Tapponnier and Molnar (1976) slip-lines model predicting geometry of strike-slip faults resulting from in-plane forces due to collision/indenter, re-drawn from faults mapping and GPS motion considering Tibet as fixed. Colors of strike-slip faults as in top panel.*